Supporting Information

The Surface Charge Induced High Activity of Oxygen Reduction Reaction on the $PdTe_2$ Bilayer

Xiang Huang,[a] Jiong Wang,[b] Changming Zhao,[a] Li-Yong Gan,[c] Hu Xu*[,a,d,e]

[a]*Department of Physics, Southern University of Science and Technology, Shenzhen 518055, China*

[b]*Innovation Center for Chemical Sciences, College of Chemistry, Chemical Engineering and Materials Science, Soochow University, Suzhou 215123, China*

[c]*Institute for Structure and Function and Department of Physics, Chongqing University, Chongqing 400030, China*

[d]*Guangdong Provincial Key Laboratory of Computational Science and Material Design, Southern University of Science and Technology, Shenzhen 518055, China*

[e]*Shenzhen Key Laboratory of Advanced Quantum Functional Materials and Devices, Southern University of Science and Technology, Shenzhen 518055, China*

*E-mail: xuh@sustech.edu.cn

Computational Details

Density functional theory calculations are carried out using the Vienna *ab initio* simulation package (VASP) interfaced with Atomic Simulation Environment (ASE).[1, 2] The interaction between ionic cores and valence electrons is described using the projector augmented wave (PAW) method.[3] The energy cutoff for the plane-wave basis is 400 eV. The PBE[4] and revised PBE[5] functionals combined with DFT-D2[6] and DFT-D3[7, 8] dispersion corrections are used to fit the lattice constant of $PdTe_2$ bulk (Table S1). Among them, the PBE-D2 derived lattice constant (a=4.02 Å, c=5.12 Å) is in excellent agreement with the experiment (a=4.04 Å, c=5.13 Å).[9] Thus, the PBE-D2 calculations are adopted throughout this work, except for the band gap calculation of $PdTe_2$ thin films, where the HSE06 hybrid functional is used.[10] The $PdTe_2$ surfaces are modelled using (2×2) and (4×4) $PdTe_2$ supercells with the vacuum layer of ~23 Å, and the Brillouin zones are sampled with Γ-centered k-meshes of 6×6×1 and 2×2×1, respectively. The dipole correction is applied to decouple the interaction between periodically repeated images. The geometrical structures are relaxed until the force on each atom is less than 0.05 eV/Å. The transition state is determined using the climbing image nudged elastic band (CI-NEB) and dimer methods with the forces converged to be less than 0.05 eV/Å.[11] The spin-polarization has been investigated for the O_2 adsorption in the interfacial model ($^{O_2^*|H^+@WL}$), and we find that it has no effect on the system (Table S2). The phonon spectrum is calculated using Phonopy code with finite difference method.[12] Considering the contributions of zero-point energy and entropy, the corrections of 0.05, 0.40, 0.05, and 0.35 eV are made for the calculated

binding energies of O_2*, OOH*, O*, and OH*, respectively.[13] The solvation energies are calculated using VASPsol.[14] It is found that O_2*, OOH*, O*, and OH* are stabilized by -0.07, -0.15, -0.13, and -0.12 eV, respectively.

Oxygen Reduction Reaction

The free energy of coupled proton-electron pair is computed based on the computational hydrogen electrode (CHE) model,[15] which derives $\mu(H^+) + \mu(e^-) = 1/2\mu(H_2) - eU$. The potential U is the electrode potential versus the reversible hydrogen electrode (RHE). The limiting potential is defined as the highest potential at which all the electrochemical steps are downhill in free energies. In this work, we consider the ORR at acid environment with pH=0. The relevant reaction steps are given in equations (1)-(4).

$$* + O_2 + H^+ + e^- \rightarrow OOH^* \quad (1)$$

$$OOH^* + H^+ + e^- \rightarrow O^* + H_2O \quad (2)$$

$$O^* + H^+ + e^- \rightarrow OH^* \quad (3)$$

$$OH^* + H^+ + e^- \rightarrow * + H_2O \quad (4)$$

where * denotes the active site on the catalyst. The free energies of O_2, *OOH, *O, and *OH at a given potential U relative to RHE are defined as

$$\Delta G(O_2) = 4.92 - 4eU$$

$$\Delta G(OOH^*) = G(OOH^*) + \frac{3G(H_2)}{2} - G(*) - 2G(H_2O) - 3eU$$

$$\Delta G(O^*) = G(O^*) + G(H_2) - G(*) - G(H_2O) - 2eU$$

$$\Delta G(OH^*) = G(OH^*) + \frac{G(H_2)}{2} - G(*) - G(H_2O) - eU$$

The Capacitor Model

If the interface is close to an ideal capacitor, ΔG_{int} will take the form

$$\Delta G_{int} = \frac{1}{2}C(U - U_{SHE})^2 + \Delta G_0$$

where C refers to the capacitance of the interface, U is the electrode potential, and U_{SHE} is an internal definition of the standard hydrogen electrode potential at which ΔG_{int} reaches the minimum ΔG_0.

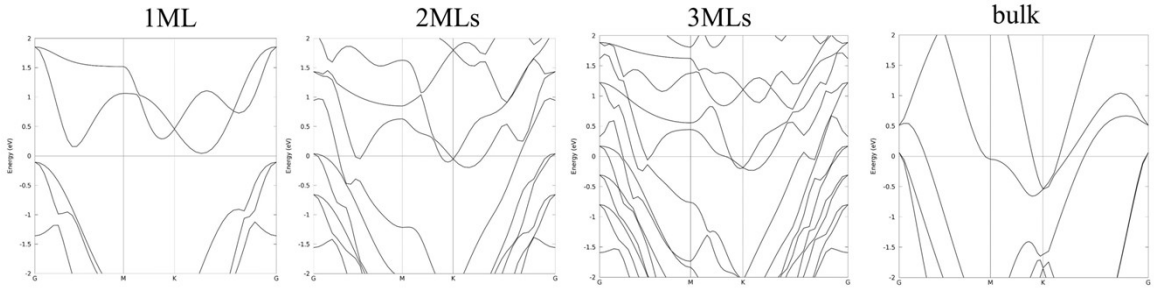

Figure S1. HSE06 calculated band structures of $PdTe_2$ with 1ML, 2MLs, and 3MLs, and of $PdTe_2$ bulk.

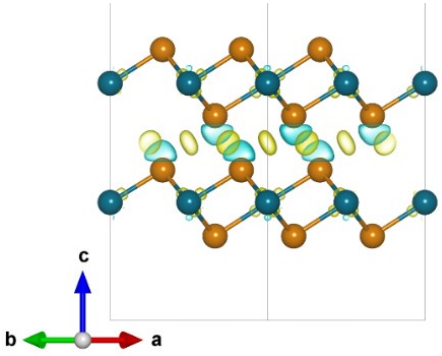

Figure S2. Charge density difference plot with isosurface of ±0.002 e/Å^3. Yellow and light green regions represent charge accumulation and depletion, respectively.

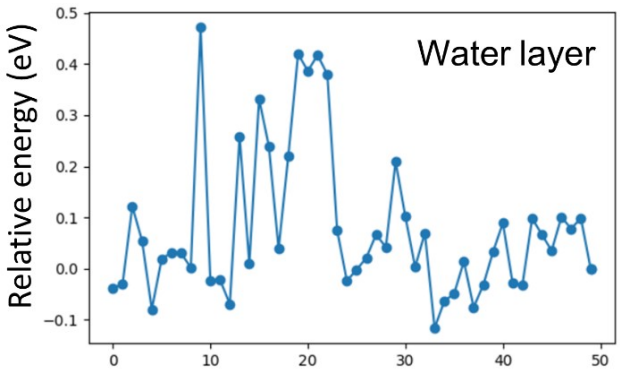

Figure S3. Relative energies of local minima of the water layer on the $PdTe_2$ bilayer determined by the minima hopping algorithm.

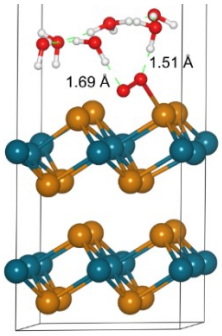

Figure S4. Geometrical configuration of $O_2^*|H^+@WL$. The lengths of hydrogen bonds formed between O_2* and interfacial H_2O molecules are indicated.

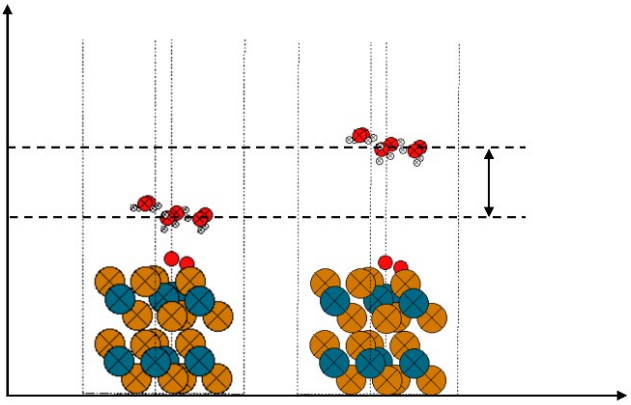

Figure S5. Schematic illustrating the regulation of the vertical height between water layer and the $PdTe_2$ surface, with the dashed lines representing the upper and lower boundaries of height. At the lower boundary of height, the distance between O_2* and nearest H_2O molecules is greater than 3 Å, thus avoiding the hydrogen bonding

interaction. The label "×" denotes the fixed atom.

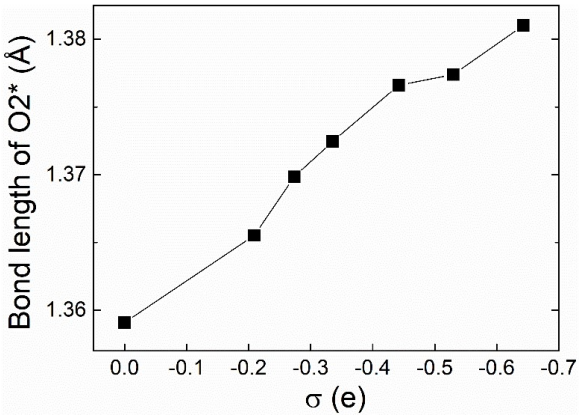

Figure S6. Bond length of O_2* plotted as a function of the charge on the $PdTe_2$ bilayer.

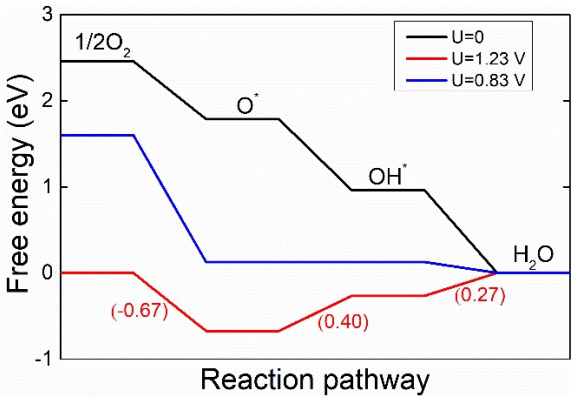

Figure S7. Free energy diagram of ORR on the $PdTe_2$ bilayer determined using the CHE model. The value in the bracket is the reaction free energy in eV at U=1.23 V.

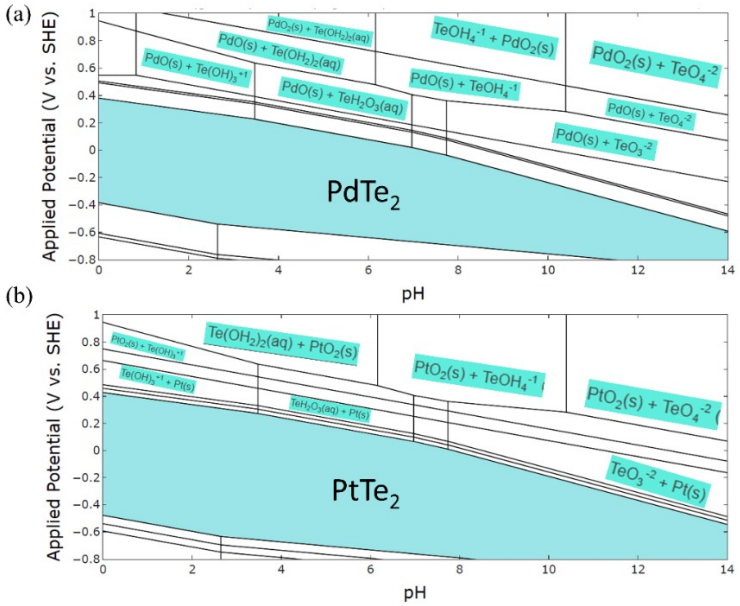

Figure S8. The Pourbaix diagrams of (a) $PdTe_2$ and (b) $PtTe_2$ produced using the DFT database in the Materials Project.[16]

Table S1. Calculated lattice constants of the $PdTe_2$ bulk using different combinations of exchange-correlation functionals and dispersion correction methods.

XC functional	Lattice constant (Å)
PBE	a= 4.10; c= 5.20
PBE-D2	a= 4.02; c= 5.12
PBE-D3 with zero damping	a=4.07; c=5.02
RPBE-D3 with zero damping	a= 4.07; c= 5.05
BEEF-vdW	a=4.13; c=5.28
Exp	a= 4.04; c= 5.13

Table S2. The DFT calculated total energies (eV) of $O_2^*|H^+@WL$ and $H^+@WL$ at different sigma values with and without spin-polarization.

Spin-unpolarized	$O_2^*\|H^+@WL$	$H^+@WL$	ΔE_{diff}
Sigma=0.2 eV	-210.207	-199.516	-10.691
Sigma=0.1 eV	-210.200	-199.520	-10.680
Sigma=0.05 eV	-210.197	-199.516	-10.682
Spin-polarized			
Sigma=0.2 eV	-210.207	-199.516	-10.690
Sigma=0.1 eV	-210.200	-199.521	-10.680
Sigma=0.05 eV	-210.197	-199.516	-10.681

References

1. G. Kresse and J. Furthmüller, *Phys. Rev. B: Condens. Matter Mater. Phys.*, 1996, **54**, 11169-11186.
2. A. Hjorth Larsen, J. Jørgen Mortensen, J. Blomqvist, I. E. Castelli, R. Christensen, M. Dułak, J. Friis, M. N. Groves, B. Hammer, C. Hargus, E. D. Hermes, P. C. Jennings, P. Bjerre Jensen, J. Kermode, J. R. Kitchin, E. Leonhard Kolsbjerg, J. Kubal, K. Kaasbjerg,

S. Lysgaard, J. Bergmann Maronsson, T. Maxson, T. Olsen, L. Pastewka, A. Peterson, C. Rostgaard, J. Schiøtz, O. Schütt, M. Strange, K. S. Thygesen, T. Vegge, L. Vilhelmsen, M. Walter, Z. Zeng and K. W. Jacobsen, *J. Phys. Condens. Matter*, 2017, **29**, 273002.

3. G. Kresse and D. Joubert, *Phys. Rev. B: Condens. Matter Mater. Phys.*, 1999, **59**, 1758-1775.
4. J. P. Perdew, K. Burke and M. Ernzerhof, *Phys. Rev. Lett.*, 1996, **77**, 3865-3868.
5. B. Hammer, L. B. Hansen and J. K. Nørskov, *Phys. Rev. B: Condens. Matter Mater. Phys.*, 1999, **59**, 7413-7421.
6. S. Grimme, *J. Comput. Chem.*, 2006, **27**, 1787-1799.
7. S. Grimme, J. Antony, S. Ehrlich and H. Krieg, *J. Chem. Phys.*, 2010, **132**, 154104.
8. S. Grimme, S. Ehrlich and L. Goerigk, *J. Comput. Chem.*, 2011, **32**, 1456-1465.
9. S. Furuseth, K. Selte and A. Kjekshus, *Acta Chem. Scand.*, 1965, **19**, 257-258.
10. J. Heyd, G. E. Scuseria and M. Ernzerhof, *J. Chem. Phys.*, 2003, **118**, 8207-8215.
11. G. Henkelman, B. P. Uberuaga and H. Jónsson, *J. Chem. Phys.*, 2000, **113**, 9901-9904.
12. A. Togo, F. Oba and I. Tanaka, *Phys. Rev. B: Condens. Matter Mater. Phys.*, 2008, **78**, 134106.
13. X. Huang, L.-Y. Gan, J. Wang, S. Ali, C.-C. He and H. Xu, *J. Phys. Chem. Lett.*, 2021, **12**, 9197-9204.
14. K. Mathew, R. Sundararaman, K. Letchworth-Weaver, T. A. Arias and R. G. Hennig, *J. Chem. Phys.*, 2014, **140**, 084106.
15. J. K. Nørskov, J. Rossmeisl, A. Logadottir, L. Lindqvist, J. R. Kitchin, T. Bligaard and H. Jonsson, *J. Phys. Chem. B*, 2004, **108**, 17886-17892.
16. A. Jain, S. P. Ong, G. Hautier, W. Chen, W. D. Richards, S. Dacek, S. Cholia, D. Gunter, D. Skinner, G. Ceder and K. A. Persson, *APL Mater.*, 2013, **1**, 011002.